Precision and Kinetics of Adaptation in Bacterial Chemotaxis

Yigal Meir,[†*] Vladimir Jakovljevic,[†] Olga Oleksiuk,[‡] Victor Sourjik,[‡] and Ned S. Wingreen[§]
[†]Department of Physics, Ben-Gurion University of the Negev, Beer Sheva, Israel; [‡]Zentrum fur Moleculare Biologie Heidelberg, University of Heidelberg, Im Neuenheimer Feld, Germany; and [§]Department of Molecular Biology, Princeton University, Princeton, New Jersey

ABSTRACT The chemotaxis network of the bacterium *Escherichia coli* is perhaps the most studied model for adaptation of a signaling system to persistent stimuli. Although adaptation in this system is generally considered to be precise, there has been little effort to quantify this precision, or to understand how and when precision fails. Using a Förster resonance energy transfer-based reporter of signaling activity, we undertook a systematic study of adaptation kinetics and precision in *E. coli* cells expressing a single type of chemoreceptor (Tar). Quantifiable loss of precision of adaptation was observed at levels of the attractant MeAsp as low 10 μM, with pronounced differences in both kinetics and precision of adaptation between addition and removal of attractant. Quantitative modeling of the kinetic data suggests that loss of precise adaptation is due to a slowing of receptor methylation as available modification sites become scarce. Moreover, the observed kinetics of adaptation imply large cell-to-cell variation in adaptation rates—potentially providing genetically identical cells with the ability to "hedge their bets" by pursuing distinct chemotactic strategies.

INTRODUCTION

Bacteria, such as *Escherichia coli*, are able to chemotaxis-up shallow gradients of attractants over a wide range of chemical concentrations. Essential to this large dynamic range of response is an adaptation system based on methylation and demethylation of chemoreceptors (1), which, in some cases, allows chemotaxis over more than four orders of magnitude of concentrations (2). Although adaptation in *E. coli* is famous for being precise, relatively little effort has been expended to quantify this precision. In particular, because adaptation is known to slow down dramatically for large stimulations, it has remained unclear whether adaptation is truly imprecise at large attractant concentrations, or merely very slow.

Here we report a systematic study of the precision and kinetics of adaptation of *E. coli* cells in response to addition and subsequent removal of attractant. Several features of our study help quantify the intrinsic precision of the network:

1. We study cells expressing a single type of receptor (Tar), eliminating the complications of ligand binding to multiple receptor types (3), and varying receptor ratios (4,5).
2. We allow long adaptation times to a nonmetabolizable attractant MeAsp, because cells can rapidly metabolize other attractants, e.g., aspartate or serine.
3. We use a Förster resonance energy transfer (FRET)-based assay (3) to characterize the chemoreceptor response upstream of the motor, which may have its own slow dynamics.

Our results reveal a systematic failure of precise adaptation beginning at concentrations as low as 10 μM of MeAsp, along with striking asymmetries in the responses to addition and subsequent removal of attractant.

The chemotaxis network of *E. coli* is one of the best characterized signal transduction networks in biology (for recent reviews focused on signaling, see (6,7)). The network consists of five types of transmembrane receptors, each of which forms homodimers. These homodimers associate in mixed "trimers of dimers" (8,9) in complex with the linker protein CheW and the kinase CheA. Trimers of dimers form ordered arrays (10), mostly at one or both cell poles. The addition of attractant biases receptor complexes to inactivate CheA (compare to Fig. 1). The removal of attractant (or the addition of repellent) activates CheA, which then uses ATP to autophosphorylate, and passes the phosphate on to the response regulator CheY or to the methylesterase CheB. Phosphorylated CheY interacts with the flagellar motor to induce clockwise rotation, resulting in tumbles or changes of swimming direction. Adaptation depends on the methyltransferase CheR, which preferentially methylates inactive receptors (11–14), and the methylesterase CheB, which preferentially demethylates active receptors. The net effect is that cells respond transiently to a change in chemoeffector concentration, but ultimately return to their original tumbling rates (or, equivalently, CheY-P levels). Theoretically, precise adaptation requires that the rates of methylation/demethylation by CheR/CheB depend only on receptor activity (1,15): because these rates must balance in steady state, and there is only one value of receptor activity for which these rates do balance, there can be only one activity level consistent with steady state—hence precise adaptation. Recently, several theoretical works have addressed the failure of precise adaptation (16,17), but until now without data suitable for direct comparison.

Experimentally, kinetic responses and adaptation have been observed in single immobilized cells (18–20), among

Submitted July 3, 2010, and accepted for publication August 18, 2010.

*Correspondence: ymeir@bgu.ac.il

Editor: Andre Levchenko.

© 2010 by the Biophysical Society

0006-3495/10/11/2766/9 $2.00

doi: 10.1016/j.bpj.2010.08.051

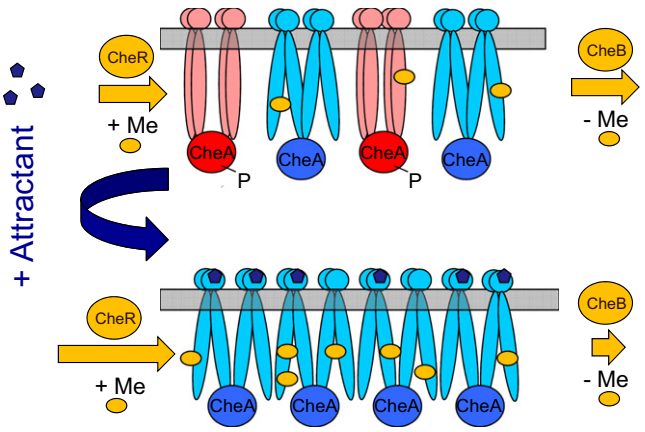

FIGURE 1 Schematic illustration of adaptation of chemotaxis receptors to addition of attractant. (*Top*) In adapted cells, the fraction of active teams of receptors is kept fixed by methylation/demethylation by CheR/CheB, respectively. Hence the fraction of CheA molecules active as kinases is also fixed, leading in swimming cells to a fixed rate of cell tumbling. (*Bottom*) Immediately after addition of attractant, signaling teams (and CheA) become inactive; CheR, which preferentially methylates inactive receptors begins working at its maximal rate, whereas CheB, which demethylates active receptors, stops working. The increased net rate of methylation eventually increases the fraction of active receptors to its initial value. In this new steady state, the increased level of receptor methylation compensates for the higher level of ambient attractant.

swimming cells (21,22), and, as in this study, upstream of the motor using CheY and its phosphatase CheZ as a FRET pair (3,4). However, none of these previous studies have systematically quantified the failure of precision of adaptation, or distinguished slow kinetics from true imprecision. The data presented here conclusively demonstrate significant loss of precise adaptation at the level of CheY-P. Aided by a quantitative model for signaling and adaptation, we interpret the loss of precise adaptation as arising from a decrease in methylation rates due to the scarcity of available sites. In addition, the detailed kinetic-response curves implicate large cell-to-cell variations in methylation/demethylation rates, with potential relevance to bet-hedging of chemotactic responses.

METHODS

Experimental techniques

Cell preparation and FRET measurements were performed as described previously (3,23). *E. coli* cells were transformed with plasmid pVS88 that mediates ampicillin resistance and encodes a CheY-YFP/CheZ-CFP FRET pair as one bicistronic construct inducible by isopropyl β-D-thiogalactoside and plasmid pVS123 that mediates chloramphenicol resistance and encodes Tar receptor, under induction by sodium salicylate (4). Cells were diluted 1:100 from overnight culture and grown to midexponential phase (OD600 $\simeq$ 0.48) at 34°C in tryptone broth (1% tryptone, 0.5% NaCl, pH 7.0) medium supplemented with 100 μg/mL ampicillin, 34 μg/mL chloramphenicol, 50 μM isopropyl β-D-thiogalactoside, and 3 μM salicylate.

For FRET measurements, cells were harvested by centrifugation, washed twice with tethering buffer (10 mM potassium phosphate, 0.1 mM EDTA, 1 mM L-methionine, 10 mM sodium lactate, pH 7.0), left for at least 30 min at 40°C, concentrated ~100-fold by centrifugation, attached to a poly-lysine-coated coverslip, and placed into a flow chamber mounted on a custom-modified inverted Axiovert 200 microscope (Carl Zeiss, Jena, Germany). Flow chamber was maintained at 25°C during all experiments. Fluorescence of a field of 300–500 cells was excited in the CFP excitation channel by a 75 XBO lamp attenuated by a ND2.6 neutral density filter and continuously recorded in CFP and YFP emission channels using photon counters (model No. H7421-40; Hamamatsu, Hamamatsu City, Japan). Constant flow (0.5 mL/min) of tethering buffer was used to add and remove specified concentrations of attractant. For each measurement point, photons were counted over one second using a counter function of PCI-6034E board, controlled by a custom-written LabView 7.1 program (both from National Instruments, Austin, TX).

Fluorescence data analysis

Each fluorescence measurement consists of data in two channels, cyan (C) and yellow (Y). To characterize receptor activity we need to know the change in the number of CheY-P:CheZ FRET pairs, $\Delta N(t)$. We expect the fluorescence in the C channel to be

$$\begin{aligned} c(t) &= S_C(t)[C_0 + N(t)\Delta C] \\ &= A_c(t)[C_0 + (N_0 + \Delta N(t))\Delta C], \end{aligned} \quad (1)$$

where $S_C(t)$ is the overall strength of the signal, which changes over time even without any change in activity. Due to bleaching, C_0 is the source of the signal when no pairs are present, ΔC is the change of the signal due to a single pair, and N_0 is the adapted number of pairs, i.e., the number of pairs before stimulation. If we know the fluorescence $c_{\mathrm{unstim}}(t)$ without chemostimulation, then we can write

$$r_c(t) = \frac{c(t) - c_{\mathrm{unstim}}(t)}{c_{\mathrm{unstim}}(t)} = \frac{\Delta C}{C_0 + N_0\Delta C}\Delta N(t), \quad (2)$$

which gives us the change in the number of pairs, $\Delta N(t)$, up to a constant factor. A parallel analysis applies to the Y channel. If consistent, then the responses $r_c(t)$ and $r_y(t)$ for the two separate channels, being both proportional to $\Delta N(t)$, should be proportional to each other, with a time-independent proportionality constant. Thus, in principle, each channel contains the same information.

To obtain the signal without chemostimulation, $c_{\mathrm{unstim}}(t)$, we fit a simple rational function to the data before stimulation and after adaptation after removal of attractant. An example is depicted in the upper inset of Fig. 2. For an accurate determination of the background, one has to continue the measurement for a substantial time after removal of attractant, allowing several hours for the higher stimulations.

Given the unstimulated signal, $c_{\mathrm{unstim}}(t)$ and $y_{\mathrm{unstim}}(t)$, we can use Eq. 2 to obtain $\Delta N(t)$ from both the C and the Y channels. As mentioned above, the responses for the two channels $r_c(t)$ and $r_y(t)$ should collapse onto each other when multiplied by some constant, which indeed holds for most of our measurements, though there is some variation in the scaling factor. There are, however, some cases where this collapse does not occur, especially for the higher stimulations. For consistency, the data presented in this article was derived from the Y channel.

MODELS

Our model for adaptation in bacterial chemotaxis follows that of Barkai and Leibler (1), generalized to allow for teams of receptors (4,24,25) that are all active or inactive together (compare to Fig. 1). This two-state model for signaling teams is closely analogous to the famous MWC model for hemoglobin (26). The basic elements of the model are:

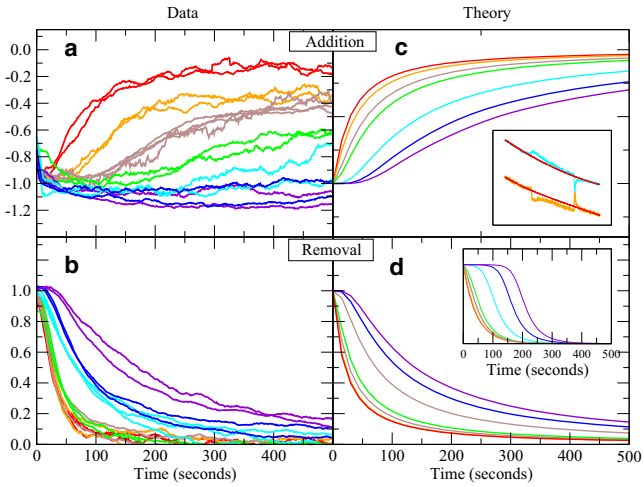

FIGURE 2 FRET data on the kinetics of adaptation after addition/removal of the attractant MeAsp to *E. coli* cells expressing only Tar receptors, and comparison with models. (*Upper inset*) Example of data analysis: to compensate for bleaching, smooth curves are fit to fluorescent output in cyan and yellow channels, taken over several hours, and receptor activity after attractant addition/removal is obtained from differences with respect to the smooth curves. (*a*) Normalized response of receptor activity to addition of steps of MeAsp, to cells adapted to zero ambient attractant. The different MeAsp concentrations are represented by different colors: 5 μM (*red*), 10 μM (*orange*), 20 μM (*light green*), 30 μM (*dark green*), 100 μM (*cyan*), 300 μM (*blue*), and 1000 μM (*purple*). (*b*) Normalized response after removal of MeAsp after adaptation to the step *a*, using the same color scale. (*Lower inset*) A minimal model for adaptation (Eqs. 3–8) incorrectly predicts large delays in adaptation after removal of higher concentrations of attractant. (*c* and *d*) A model for adaptation including cell-to-cell variation in CheRB concentrations (Eq. 9) accounts well for removal data, but fails to account for the observed slow and incomplete adaptation after attractant addition.

1. A free-energy model for the probability that a team will be active, depending on the methylation level of the receptors and the concentration of ligand.
2. A kinetic model for the rate of change of the receptor methylation level due to the enzymes CheR and CheB.

In the free-energy model for teams composed of a single receptor type, e.g., Tar, the probability A that the team will be active is

$$A = \frac{1}{1 + e^{n_r f}}, \tag{3}$$

where n_r is the number of receptor homodimers in a team and f is the free-energy difference between active and inactive states of one receptor dimer,

$$f = f_0 + \log\left[\left(1 + [\mathrm{L}]/K_{\mathrm{off}}\right)/\left(1 + [\mathrm{L}]/K_{\mathrm{on}}\right)\right] + f'_m m, \tag{4}$$

with f_0 the free-energy difference in the absence of ligand, [L] the ligand concentration, and $K_{\mathrm{on/off}}$ the receptor-ligand dissociation constants in the active (on) and inactive (off) states. For a chemoattractant, $K_{\mathrm{off}} < K_{\mathrm{on}}$. For simplicity, the free-energy difference is assumed to depend linearly on the receptor dimer methylation level, $m = 0,\ldots 8$, with a coefficient $f'_m < 0$ (21,27). All energies are expressed in units of the thermal energy, $k_B T$.

For the kinetics of methylation, we assume a mean-field form of the Barkai-Leibler formula in which CheR only methylates inactive receptors and CheB only methylates active receptors,

$$\frac{dm(t)}{dt} = \gamma_R[1 - A(t)] - \gamma_B A(t), \tag{5}$$

where $m(t)$ is the mean methylation level per receptor dimer at time t, and γ_R and γ_B are the maximal methylation and demethylation rates, respectively. Because the activity at fixed ligand concentration is purely a function of the methylation level, we obtain a mean-field formula for the activity,

$$\frac{dA(t)}{dt} = \frac{dA}{dm}[\gamma_R - (\gamma_B + \gamma_R)A(t)]. \tag{6}$$

Within the free-energy model (4),

$$\frac{dA}{dm} = -f'_m n_r A(1 - A), \tag{7}$$

leading to

$$\begin{aligned} \tfrac{dA(t)}{dt} &= -f'_m n_r A(t)[1 - A(t)][\gamma_R - (\gamma_B + \gamma_R)A(t)] \\ &= -\gamma A(t)[1 - A(t)][A(t) - A^*], \end{aligned} \tag{8}$$

where

$$A^* \equiv \gamma_R/(\gamma_B + \gamma_R)$$

is the adapted value of A, and

$$\gamma \equiv \left|f'_m\right| n_r(\gamma_B + \gamma_R).$$

$1/\gamma$ defines the timescale for adaptation.

Distribution of CheR and CheB levels

From the experimental data on adaptation kinetics, we infer a significant cell-to-cell variation in CheR and CheB (CheRB) levels. In theory, stochastic gene expression leads to a γ-distribution of protein levels (28,29). We therefore model variation in CheRB levels by assuming such a γ-distribution for the adaptation-rate parameter γ (while keeping the ratio γ_R/γ_B fixed because CheR and CheB are expressed from the same operon),

$$p(\gamma; a, b) = \frac{1}{b^a \Gamma(a)} \gamma^{a-1} e^{-\gamma/b}, \tag{9}$$

where $\Gamma(a)$ is the γ-function. Note that the two parameters a and b in the γ-distribution $p(\gamma; a, b)$ define its mean, ab, and its variance, ab^2.

Dynamic phosphorylation of CheB

One part of the adaptation process that is inherently asymmetric between addition and removal of attractant is CheB phosphorylation. Like CheY, CheB is phosphorylated by

CheA, and CheB-P is ~70-fold more active than CheB in demethylating receptors (30). Therefore, as the receptor activity increases, more CheB is phosphorylated by CheA, leading to a higher maximal rate of demethylation. If we assume simple first-order kinetics for CheB phosphorylation/dephosphorylation,

$$\frac{d[\mathrm{CheB-P}](t)}{dt} = \alpha A(t)[\mathrm{CheB}] - \mu[\mathrm{CheB-P}], \quad (10)$$

and further assume that CheB-P levels respond quickly to receptor activity, then

$$[\mathrm{CheB-P}](t) \simeq \frac{\alpha A(t)}{\alpha A(t) + \mu}[\mathrm{CheB}]_{\mathrm{total}}, \quad (11)$$

implying that the demethylation rate $\gamma_B(t)$ follows the activity $A(t)$. For simplicity, we assume [CheB-P] remains in the linear regime with respect to $A(t)$, yielding a new term in the kinetic equation for receptor methylation (5):

$$\frac{dm(t)}{dt} = \gamma_R[1 - A(t)] - \left[\gamma_B + \gamma'_B A(t)\right]A(t). \quad (12)$$

Because the right-hand side is only a function of $A(t)$, one still expects perfect adaptation, though the adapted activity value will now depend on γ_R, γ_B, and γ'_B.

Failure of precise adaptation due to scarcity of methylation sites

Another part of the adaptation process that is asymmetric between addition and removal of attractant is the availability of methylation sites. Upon addition of attractant, methylation increases and available modification sites become more scarce, which may slow down the rate of further methylation. We can model the effect of scarce methylation sites by introducing a saturation factor N_0 (17), which can be thought of as a number of effective "dead sites" where CheR can reside but cannot methylate. Because CheR acts within an "assistance neighborhood" of $S_{\mathrm{AN}} \sim 6$ receptor dimers (31), the total number of modification sites is $8S_{\mathrm{AN}} \sim 48$, and the effect of scarce sites only becomes important when the available sites in a neighborhood drops to $\sim N_0$. In the presence of this saturation factor N_0, the kinetic equation (Eq. 5) for the mean methylation level becomes

$$\frac{dm(t)}{dt} = \gamma_R \frac{N_a(t)}{N_a(t) + N_0}[1 - A(t)] - \gamma_B A(t), \quad (13)$$

where N_a is the number of available methylation sites in an assistance neighborhood. If $M_{\mathrm{tot}} = 8S_{\mathrm{AN}}$ is the total number of methylation sites in the neighborhood, then $N_a(t) = M_{\mathrm{tot}} - M(t)$, where $M(t) = m(t)\,S_{\mathrm{AN}}$ for an assistance neighborhood of S_{AN} receptors. Within this scarce-methylation-site model, the steady-state (adapted) activity A_0^* obeys

$$\gamma_B/\gamma_R = \frac{M_{\mathrm{tot}} - M_0}{M_{\mathrm{tot}} - M_0 + N_0}\frac{1 - A_0^*}{A_0^*}, \quad (14)$$

where $M_0 = m_0 S_{\mathrm{AN}}$ is the initial methylation level of the neighborhood, with m_0 the initial methylation level per receptor. Using Eqs. 3 and 4, we can write

$$m(t) - m_0 = \frac{1}{f'_m}\Bigg[-\log\left[\left(1 + [\mathrm{L}]/K_{\mathrm{off}}\right)/\left(1 + [\mathrm{L}]/K_{\mathrm{on}}\right)\right] + \frac{1}{n_r}\log\frac{1 - A(t)}{A(t)} - \frac{1}{n_r}\log\frac{1 - A_0^*}{A_0^*}\Bigg]. \quad (15)$$

Thus Eq. 13 implies

$$\frac{dA(t)}{dt} = -f'_m n_r A(t)[1 - A(t)] \times \left\{\gamma_R \frac{N_a(t)}{N_a(t) + N_0}[1 - A(t)] - \gamma_B A(t)\right\}, \quad (16)$$

with $N_a(t) = M_{\mathrm{tot}} - M(t)$ obtained from Eq. 15.

Parameters

Except where noted, we used the following parameters: $K_{\mathrm{off}} = 25\ \mu$M and $K_{\mathrm{on}} = 500\ \mu$M for Tar receptors binding MeAsp (25), the team size $n_r = 5$ (4,32), and the adapted activity $A^* = 1/3$ (3). Unless otherwise mentioned, the parameters characterizing the CheRB distribution were taken to be $a = 1.2$ and $b = 0.05\ \mathrm{s}^{-1}$. The qualitative results are insensitive to the exact parameter choices.

RESULTS

FRET data reveal qualitative differences between responses to addition/removal of attractant

Data on the kinetic response of receptor activity to step addition and removal of attractant are shown in Fig. 2, *a* and *b*. Receptor kinase activity in *E. coli* cells expressing only Tar receptors was assayed using the FRET pair consisting of CheY and its phosphatase CheZ, which form heterodimers only when CheY is phosphorylated. The rate of dephosphorylation of CheY-P by CheZ is in rapid quasiequilibrium with the rate of phosphorylation of CheY by CheA (compare to Fig. 1). Therefore the concentration of CheY-P:CheZ pairs measured by FRET is proportional to the kinase activity of the receptor complexes, i.e., the probability that receptor teams are active. To generate each curve in Fig. 2, *a* and *b*, a step of concentration of the attractant MeAsp was applied by flow at $t = 0$ to cells adapted to zero ambient MeAsp, and the cells were then allowed to fully adapt before the MeAsp was removed. An example of the raw data, with the compensation for bleaching, is shown in the upper inset of Fig. 2. Because of day-to-day variations in overall FRET amplitudes, the response curves for different MeAsp concentrations were normalized to the same peak response amplitude, which allows for easy comparison of adaptation kinetics.

There are evident differences between the kinetic responses to addition and removal of MeAsp in Fig. 2, *a* and *b*. First, the responses are clearly not symmetric. The characteristic time for adaptation after addition is always longer than the time required for adaptation after removal. Second, the removal curves collapse onto each other for low stimulations (small steps of MeAsp concentration), indicating a single relaxation time, and this time increases only modestly for large stimulations. In contrast, the adaptation time after addition strongly increases with stimulation size, starting from the smallest stimulations. Lastly, the addition curves fail to adapt completely at higher stimulations, asymptotically approaching adapted activities lower than the prestimulation activity at long times. In what follows, we attempt to account for these observations within the standard model for adaptation. Our conclusions are that CheB phosphorylation contributes to the asymmetry between the addition and removal curves, but that the data also imply substantial cell-to-cell variations in CheRB concentrations and a slowing of the rate of methylation as available modification sites become scarce.

Adaptation kinetics indicate large cell-to-cell variation in methylation/demethylation rates

It is useful to first compare the removal curves shown in Fig. 2 *b* to results from a minimal model for adaptation shown in the lower inset of Fig. 2. Within the model (Eq. 8, with $\gamma = 0.03$ 1/s), removal of MeAsp results in an instant upshift of receptor activity, followed by adaptation of the activity precisely back to its original level via progressive demethylation of the receptors by CheB. Increasing the stimulus size results in an increased delay before the activity starts to drop, but then all curves drop at the same rate, i.e., the response curves for different stimulations are essentially just shifted in time. In contrast, the experimental curves shown in Fig. 2 *b* collapse for small stimulus sizes, and, for large stimulus sizes, instead of being shifted in time, the curves relax more slowly to the original activity. How can we understand these discrepancies between theory and experiment? We will argue below that these discrepancies can be accounted for by cell-to-cell variations in the concentrations of CheR and CheB. First, however, it is helpful to examine the behavior expected from the naive application of the standard model (Eq. 8).

In the free-energy model for receptor activity, entire teams of receptors are either active or inactive together with a probability set by thermal equilibrium (compare to Eqs. 3 and 4). The team free-energy difference ΔF between active and inactive states depends additively on contributions from methylation, which favors the active state, and ambient attractant concentration, which favors the inactive state. Starting at zero ambient concentration, addition of attractant shifts ΔF to a positive value, favoring inactive receptors. For a large enough step of attractant, the resulting rise in ΔF will be large compared to the thermal energy k_BT, and the receptors will become $\simeq 100\%$ inactive.

In the model, CheR only methylates inactive receptors and CheB only methylates active receptors, so after an attractant step the rate of methylation increases and the rate of demethylation decreases, resulting in increased net methylation. This addition of methyl groups shifts ΔF back toward its original value, with adaptation ceasing when the rates of methylation and demethylation come back into balance. Essentially the opposite then occurs after removal of attractant—the receptors are now more methylated so that removal results in a negative ΔF, favoring active receptors. The resulting changes in the rates of methylation/demethylation lead to demethylation, and adaptation continues until the receptors have again returned to their original activity level.

Within this simple model, the behavior seen in the lower inset to Fig. 2 is easily understood. After removal of a small step of attractant, ΔF is negative but not much larger in magnitude than k_BT. The receptors are therefore $<100\%$ active, and demethylation immediately results in an observable decrease of activity. However, after removal of a large concentration of attractant, ΔF becomes very negative, receptors are $\simeq 100\%$ active, and a period of progressive demethylation is required to raise ΔF enough for the activity to drop noticeably. Moreover, within this model, the curves for different step sizes are necessarily identical up to a time shift, because for all curves the ambient attractant concentration is the same (zero) and therefore the only dynamic variable is the methylation level. With only one variable, there can only be one adaptation curve, with the differences for different stimulation levels residing in the initial level of receptor methylation.

In contrast to this prediction of the simple model, the experimental removal curves in Fig. 2 *b* begin adapting almost immediately, even for the largest attractant steps. For step removal of 300 μM MeAsp and above, receptor activity approaches saturation, as judged by absolute FRET levels (see Fig. S1 in the Supporting Material), so one cannot attribute the rapid response to failure to approach 100% activity. Instead, we infer a substantial cell-to-cell variation in the level of CheB among the 300–500 cells in the FRET field of view. In those cells with high CheB levels, the response to removal is very rapid because the maximum rate of demethylation is high. However, there are also cells in the population with low CheB levels, which adapt slowly. As shown in Fig. 2 *d*, the overall effect of adding a broad distribution of CheB levels to the model is a rapid initial response to attractant removal followed by a much slower approach to the final adapted activity level, matching well the experimental curves in Fig. 2 *b*. To generate the modeling curves in Fig. 2 *d*, we used Eq. 8 with a γ-distribution of the adaptation-rate parameter γ (see Models) reflecting variation in CheRB levels due to stochastic gene expression. Because CheR and CheB are expressed from

the same operon, we assumed for simplicity that the ratio of the concentrations of CheR and CheB remains the same, independent of expression level, leading to the same adapted activity level for all cells.

Although a broad distribution of CheRB levels accounts well for the kinetics of adaptation after attractant removal, there are clear differences between the experimental and model results for the kinetics after addition. In particular, by using the same parameters obtained from the good fit to the removal data, the very long adaptation times and failure of precise adaptation for large stimulations that are seen experimentally in Fig. 2 *a* are not reproduced by the model in Fig. 2 *b*.

Sources of asymmetry between addition and removal curves

There are two likely possible sources of asymmetry between the kinetic responses to addition and removal of attractant:

1. Dynamic phosphorylation of CheB.
2. Scarcity of methylation sites.

We first consider the role of CheB phosphorylation by CheA. CheB-P is ~70-fold more active as a demethylase than CheB (30), which makes the maximal demethylation rate strongly dependent on overall receptor activity. For strong stimulations, this creates an asymmetry between addition and removal. After addition, CheR slowly methylates receptors leading to slow adaptation, whereas after removal, CheB-P rapidly demethylates receptors leading to fast adaptation. The effects of dynamic CheB phosphorylation can be easily included in our simple model for methylation kinetics (see Eq. 12 in Models). The inclusion of CheB phosphorylation results in significantly faster adaptation after removal, without significant change in the shape of the curves (see Fig. S2). Thus, in order to fit the experimental curves, the parameter b, defining the scale of the rate parameter γ (Eq. 9), was chosen to be slower, $b = 0.015\ s^{-1}$. This change of scale leads to an apparent slowing down of the response to addition and to significant asymmetry between addition and removal (see Fig. 3). However, CheB phosphorylation does not explain the experimentally observed failure of precise adaptation after addition of attractant, which implicates instead the other source of asymmetry—methylation-site scarcity.

Each Tar homodimer has eight glutamate residues that can be reversibly methylated/demethylated by CheR/CheB, respectively. Failure of precise adaptation occurs if the rate of methylation/demethylation depends on the number of available modification sites (1,17). For example, after a large step of attractant, adaptation requires a substantial increase of the receptor methylation level. If the rate of methylation slows down as available sites become filled, then the effective rate of methylation will decrease, leading to an overall lower adapted activity level. Within the simple model, the adapted activity A^* is equal to $\gamma_R/(\gamma_B + \gamma_R)$, so a decrease in the methylation rate γ_R leads directly to a decrease in the adapted activity. In contrast, after removal of attractant, the final adapted state must be identical to the original prestimulation adapted state, because the conditions are identical. Therefore, after removal the activity must return precisely to its original value.

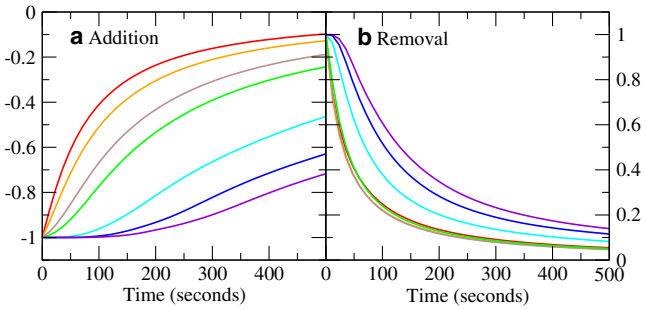

FIGURE 3 Effect of CheB phosphorylation on model adaptation kinetics. (*a*) Normalized responses to addition of steps of attractant of different amplitudes (same color-code as in Fig. 2), including dynamical CheB phosphorylation (Eq. 12, with $\gamma_B/\gamma_R = 3$ and $\gamma'_B/\gamma_R = 5$; all other parameters unchanged). (*b*) Normalized responses to removal of attractant after adaptation to the step in panel *a*, using the same color code. Increased CheB phosphorylation speeds-up adaptation after removal of attractant, but precise adaptation is retained.

To model, quantitatively, the effect of methylation-site scarcity on the kinetics of adaptation, we introduce a saturation factor N_0 (17) that can be regarded as a number of dead sites where CheR can reside without transferring a methyl group (see Models). As the number of available sites drops to ~N_0, the effective methylation rate slows down dramatically. As shown in Fig. 4 *a*, this slowing of the rate of methylation leads to incomplete adaptation, which becomes more pronounced at larger stimulation levels. As expected, there is no failure of precise adaptation after removal, as seen in Fig. 4 *b*. In Fig. 4, *c* and *d*, we show the expected dynamics of methylation after addition and then removal of attractant. The failure of precise adaptation after addition of large concentrations of attractant corresponds to the near-saturation of all available methylation sites. How strongly does the value of the initial activity affect the precision of adaptation? By changing the ratio γ_R/γ_B we can change the initial activity A_0^* in the model. Interestingly, as shown in the inset to Fig. 4 *d*, when scaled by the initial activity A_0^*, the precision of adaptation as a function of added attractant is almost independent of A_0^* over the physiological range from $A_0^* = 0.2$–0.8.

DISCUSSION

In *E. coli* chemotaxis, changes in external chemical concentration lead to changes in the activity of teams of receptors, and, ultimately, control the rate of motor switching and cell tumbling. Without adaptation, receptors could respond only over a narrow range of concentrations, being either fully

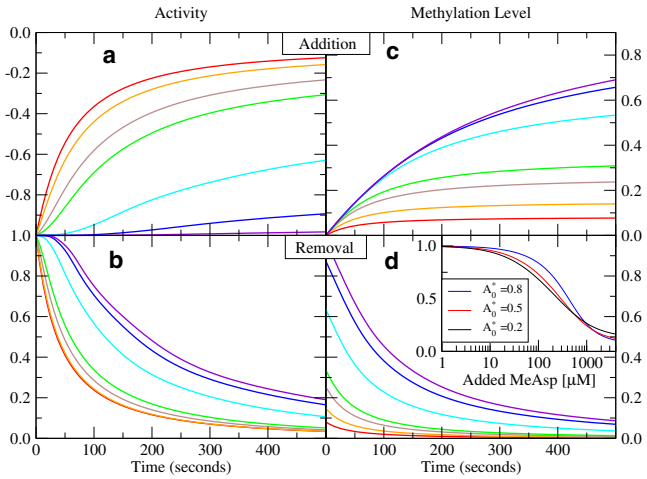

FIGURE 4 Effect of scarcity of methylation sites on model adaptation kinetics. (*a*) Normalized responses to addition of steps of attractant of different amplitudes (same color-code as in Fig. 2), including scarcity of methylation sites (Eqs. 13–16). Scarcity of methylation sites slows adaptation after addition of attractant and causes deviations from precise adaptation. (*b*) Normalized responses to removal of attractant after adaptation to the step in panel *a*, using the same color-code. (*c*) Dynamics of change in methylation level after addition of attractant, using the same color-code as in panel *a*. Curves show $(m(t) - m_0)/(m_{tot} - m_0)$, where $m(t)$ is the mean receptor methylation, with number of methylated sites in an assistance neighborhood of S_{AN} receptors, m_0 is the initial methylation level per receptor (before addition of attractant), and m_{tot} (= 8) is the total number of methylation sites in a receptor dimer. (*d*) Dynamics of methylation level after removal of attractant from fully adapted cells. The parameters used to generate these curves were $f'_m N_0/S_{AN} = -4$ and $f'_m(m_{tot} - m_0) = -2$. All other parameters are the same as before. (*Inset*) Precision of adaptation, quantified by the ratio of final activity to initial activity, after addition of MeAsp for different values of initial activity, $A_0^* = 0.2, 0.5, 0.8$. (For details, see Models.)

active or fully inactive outside this range. Instead, adaptation by reversible methylation/demethylation of the receptors allows cells to navigate shallow chemical gradients over many orders-of-magnitude of chemical concentration (2). This adaptation system represents an elegant example of integral feedback control (1,15). Theoretically, adaptation will be precise—i.e., returning receptors to precisely the same mean activity level for any constant external chemoeffector concentration—as long as the methylation/demethylation rates depend only on receptor activity. However, these rates could also depend on chemoeffector concentrations or the number of available modification sites, leading to deviations from precise adaptation (17), but until now (to our knowledge) such deviations have not been systematically explored. Here, we used a FRET-based assay to measure in vivo receptor activity in response to addition and removal of different concentration steps of the attractant MeAsp. By virtue of long measurement times, we were able to disentangle the (slow) kinetics of adaptation from the precision of adaptation, with the following conclusions:

1. Adaptation is significantly imprecise starting at concentrations as low as 10 μM MeAsp.
2. Phosphorylation of the methylesterase CheB accounts for the fast adaptation observed after removal of attractant.
3. There is considerable cell-to-cell variation in adaptation rates, implying large variations in CheR and CheB levels.

In models for chemoreceptor signaling, precise adaptation requires that the rates of receptor methylation by CheR and demethylation by CheB depend only on receptor activity. There is considerable experimental evidence that CheR preferentially methylates receptors that are in an inactive configuration (11–14), and the CheB preferentially demethylates receptors that are in an active configuration. However, this does not rule out additional dependencies of these rates on other factors. In particular, it would be natural for the rate of methylation/demethylation to depend on the number of available modification sites. Certainly, when there are no sites available, the rate of methylation/demethylation must be zero, independent of receptor activity. Interestingly, CheR and CheB tether to specific sequences at the C-terminal tails of chemoreceptors and are then able to methylate/demethylate within assistance-neighborhoods of ~6 receptor homodimers (31). Therefore the total number of sites within reach of a single tethered CheR or CheB is $\sim 6 \times 8 = 48$, so that as long as the mean methylation level per dimer is not very close to its limits (0 or 8), the probability of CheR or CheB finding no available sites by chance is very small (16). However, as the mean methylation level approaches one of these limits, there will typically be only a few available sites for either CheR or CheB within a neighborhood. Under these circumstances, the dead time spent by CheR or CheB not bound to an available site might become significant. This effect has been modeled theoretically (17) by introducing a saturation factor, equivalent to additional effective dead sites, where CheR/CheB can reside but not methylate/demethylate. The net result of these dead sites is a slowing of methylation or demethylation as the receptors approach the corresponding saturated limits, with the consequence of marked deviations from precise adaptation. The model for adaptation including dead sites was able to account for the observed failure of precise adaptation at modest concentrations of serine (~10 μM) for wild-type swimming cells, even though the same cells adapted precisely to aspartate concentrations up to 10 mM (2), the difference arising from a 2:1 ratio of serine-sensitive Tsr receptors to aspartate-sensitive Tar receptors.

Here we found that the same dead-site model can quantitatively explain the dose-dependence of the loss of adaptation precision in response to MeAsp. Why, in this study, did deviations from precise adaptation occur at concentrations of MeAsp as low as 10 μM, whereas in wild-type cells no such deviations were observed for aspartate concentrations as high as 10 mM (2)? The explanation cannot be the different affinities for the two ligands, because Tar receptors have lower affinity for MeAsp than aspartate, which would tend to make adaptation more precise to

MeAsp than to aspartate (because the free-energy change per receptor would be lower for MeAsp). According to our model, the explanation lies in the fact that the cells in our study express only Tar receptors. As a result, addition of MeAsp changes the free-energy difference of all receptors. In contrast, in wild-type cells Tars may account for only ~1/4 of receptors in a signaling team, reducing ΔF of the team as a whole by the same factor. Consequently, the degree of methylation required to compensate for the addition of attractant is smaller, and the signaling teams in wild-type cells exposed to aspartate never approach the limit of full methylation (16).

The physiological significance of CheB phosphorylation in *E. coli* chemotaxis remains an open question. Cells expressing only a nonphosphorylatable truncation of CheB still display precise adaptation (22). It has recently been suggested that CheB phosphorylation buffers the adapted level of CheY-P to fluctuations in CheR, CheB, and other chemotaxis protein levels (33). Our studies confirm that adaptation after removal of attractant is much faster than adaptation after addition of attractant for large stimulations, consistent with a large increase in CheB-P levels and demethylase activity in cells with highly active receptors. However, for small stimulations, in the regime of linear response, there can, in principle, be no asymmetry between addition and removal. Therefore, at least for cells navigating shallow gradients where typical stimulation amplitudes are small, there will be no asymmetry of response to swimming up, versus down, gradient (other than the overall sign). Moreover, if accelerated adaptation to large stimulations was physiologically important, one might have expected a similar activity-dependent modification of CheR to accelerate methylation rates. We conclude that the asymmetry of response to large stimulations is likely a byproduct of a system designed for some other function, e.g., to provide robust adapted CheY-P levels, for which homeostatic regulation of the activity of only one of the adaptation enzymes is required (33).

An important conclusion from our analysis is that there is large cell-to-cell variation in adaptation rates. The cells in our study are genetically identical, have the same growth history, and are exposed to the same chemical environment in our flow cell. Thus, the variation in adaptation rates must represent intrinsic stochasticity within the chemotaxis network. A previous study of motor switching in single cells revealed slow variation of switching rates, which were traced to fluctuations due to the small number of CheR proteins (34). Because in *E. coli* the *cheR*, *cheB*, and *cheY* genes are adjacent on an operon, variations of the three protein levels are expected and observed to be correlated (35). The correlation between CheB and CheY allows an estimate of CheB fluctuations based on observed CheY variation. Specifically, in wild-type cells the variation of CheY levels was observed to be 67% (33), which is roughly consistent with our inferred variation of

$$1/\sqrt{a} = 1/\sqrt{1.2} \simeq 90\%$$

in demethylation rates, assuming these arise from variation in CheB levels ($1/\sqrt{a}$ is the relative variation of the γ-distribution, Eq. 9). This range of variation is also roughly consistent with Berg and Tedesco's (18) observation of 48% cell-to-cell variation in adaptation times after addition of 1 mM MeAsp to wild-type cells, which implies a ~50% variation in CheR levels. Indeed, coupled variation of CheB and CheR levels has been argued to provide a robust adapted level of CheY-P (35), within the sensitive response range of the motor (36), while still allowing for large variation in adaptation rates. What role might variable adaptation rates play? The rate of adaptation is an important control variable in determining chemotactic efficiency in different-sized gradients (37), so variation in this rate could represent a bet-hedging strategy (38), with different cells in a population optimally prepared for a range of different chemical gradients.

In summary, our quantitative study of adaptation precision in *E. coli* coupled with modeling analysis has provided additional insights into the operation of the chemotaxis network of bacteria. We expect that quantitative experimental approaches with close coupling to theory will continue to yield new insights into this and other cellular signaling networks.

SUPPORTING MATERIAL

Two figures are available at http://www.biophysj.org/biophysj/supplemental/S0006-3495(10)01047-7.

Y.M., V.S., and N.S.W. acknowledge the hospitality of the Aspen Center for Physics.

This work was supported in part by the Human Frontier Science Program and grant No. GM082938 from the National Institutes of Health, Bethesda, MD.

REFERENCES

1. Barkai, N., and S. Leibler. 1997. Robustness in simple biochemical networks. *Nature.* 387:913–917.
2. Berg, H. C., and D. A. Brown. 1972. Chemotaxis in *Escherichia coli* analyzed by three-dimensional tracking. *Nature.* 239:500–504.
3. Sourjik, V., and H. C. Berg. 2002. Receptor sensitivity in bacterial chemotaxis. *Proc. Natl. Acad. Sci. USA.* 99:123–127.
4. Sourjik, V., and H. C. Berg. 2004. Functional interactions between receptors in bacterial chemotaxis. *Nature.* 428:437–441.
5. Salman, H., and A. Libchaber. 2007. A concentration-dependent switch in the bacterial response to temperature. *Nat. Cell Biol.* 9:1098–1100.
6. Sourjik, V. 2004. Receptor clustering and signal processing in *E. coli* chemotaxis. *Trends Microbiol.* 12:569–576.
7. Hazelbauer, G. L., J. J. Falke, and J. S. Parkinson. 2008. Bacterial chemoreceptors: high-performance signaling in networked arrays. *Trends Biochem. Sci.* 33:9–19.
8. Ames, P., C. A. Studdert, …, J. S. Parkinson. 2002. Collaborative signaling by mixed chemoreceptor teams in *Escherichia coli*. *Proc. Natl. Acad. Sci. USA.* 99:7060–7065.

9. Studdert, C. A., and J. S. Parkinson. 2004. Crosslinking snapshots of bacterial chemoreceptor squads. *Proc. Natl. Acad. Sci. USA.* 101: 2117–2122.
10. Briegel, A., H. J. Ding, …, G. J. Jensen. 2008. Location and architecture of the *Caulobacter crescentus* chemoreceptor array. *Mol. Microbiol.* 69:30–41.
11. Stock, J. B., and D. E. Koshland, Jr. 1981. Changing reactivity of receptor carboxyl groups during bacterial sensing. *J. Biol. Chem.* 256:10826–10833.
12. Terwilliger, T. C., J. Y. Wang, and D. E. Koshland, Jr. 1986. Kinetics of receptor modification. The multiply methylated aspartate receptors involved in bacterial chemotaxis. *J. Biol. Chem.* 261:10814–10820.
13. Shapiro, M. J., D. Panomitros, and D. E. Koshland, Jr. 1995. Interactions between the methylation sites of the *Escherichia coli* aspartate receptor mediated by the methyltransferase. *J. Biol. Chem.* 270: 751–755.
14. Amin, D. N., and G. L. Hazelbauer. 2010. The chemoreceptor dimer is the unit of conformational coupling and transmembrane signaling. *J. Bacteriol.* 192:1193–1200.
15. Yi, T.-M., Y. Huang, …, J. Doyle. 2000. Robust perfect adaptation in bacterial chemotaxis through integral feedback control. *Proc. Natl. Acad. Sci. USA.* 97:4649–4653.
16. Endres, R. G., and N. S. Wingreen. 2006. Precise adaptation in bacterial chemotaxis through "assistance neighborhoods". *Proc. Natl. Acad. Sci. USA.* 103:13040–13044.
17. Hansen, C. H., R. G. Endres, and N. S. Wingreen. 2008. Chemotaxis in *Escherichia coli*: a molecular model for robust precise adaptation. *PLOS Comput. Biol.* 4:e1.
18. Berg, H. C., and P. M. Tedesco. 1975. Transient response to chemotactic stimuli in *Escherichia coli*. *Proc. Natl. Acad. Sci. USA.* 72: 3235–3239.
19. Segall, J. E., S. M. Block, and H. C. Berg. 1986. Temporal comparisons in bacterial chemotaxis. *Proc. Natl. Acad. Sci. USA.* 83:8987–8991.
20. Tu, Y., T. S. Shimizu, and H. C. Berg. 2008. Modeling the chemotactic response of *Escherichia coli* to time-varying stimuli. *Proc. Natl. Acad. Sci. USA.* 105:14855–14860.
21. Shimizu, T., Y. Tu, and H. C. Berg. 2010. A modular gradient-sensing network for chemotaxis in *Escherichia coli* revealed by responses to time-varying stimuli. *Mol. Syst. Biol.* 6:382.
22. Alon, U., M. G. Surette, …, S. Leibler. 1999. Robustness in bacterial chemotaxis. *Nature.* 397:168–171.
23. Sourjik, V., A. Vaknin, …, H. C. Berg. 2007. In vivo measurement by FRET of pathway activity in bacterial chemotaxis. *Methods Enzymol.* 423:365–391.
24. Mello, B. A., and Y. Tu. 2005. An allosteric model for heterogeneous receptor complexes: understanding bacterial chemotaxis responses to multiple stimuli. *Proc. Natl. Acad. Sci. USA.* 102:17354–17359.
25. Keymer, J. E., R. G. Endres, …, N. S. Wingreen. 2006. Chemosensing in *Escherichia coli*: two regimes of two-state receptors. *Proc. Natl. Acad. Sci. USA.* 103:1786–1791.
26. Monod, J., J. Wyman, and J. P. Changeux. 1965. On the nature of allosteric transitions: a plausible model. *J. Mol. Biol.* 12:88–118.
27. Endres, R. G., J. J. Falke, and N. S. Wingreen. 2007. Chemotaxis receptor complexes: from signaling to assembly. *PLOS Comput. Biol.* 3:e150.
28. Friedman, N., L. Cai, and X. S. Xie. 2006. Linking stochastic dynamics to population distribution: an analytical framework of gene expression. *Phys. Rev. Lett.* 97:168302.
29. Cai, L., N. Friedman, and X. S. Xie. 2006. Stochastic protein expression in individual cells at the single molecule level. *Nature.* 440: 358–362.
30. Anand, G. S., P. N. Goudreau, and A. M. Stock. 1998. Activation of methylesterase CheB: evidence of a dual role for the regulatory domain. *Biochemistry.* 37:14038–14047.
31. Li, M., and G. L. Hazelbauer. 2005. Adaptational assistance in clusters of bacterial chemoreceptors. *Mol. Microbiol.* 56:1617–1626.
32. Hansen, C. H., Y. Meir, …, N. S. Wingreen. 2008. Variable sizes of *Escherichia coli* chemoreceptor signaling teams. *Mol. Syst. Biol.* 4:1–9.
33. Kollmann, M., L. Løvdok, …, V. Sourjik. 2005. Design principles of a bacterial signaling network. *Nature.* 438:504–507.
34. Korobkova, E., T. Emonet, …, P. Cluzel. 2004. From molecular noise to behavioral variability in a single bacterium. *Nature.* 428:574–578.
35. Løvdok, L., K. Bentele, …, V. Sourjik. 2009. Role of translational coupling in robustness of bacterial chemotaxis pathway. *PLoS Biol.* 7:e1000171.
36. Cluzel, P., M. Surette, and S. Leibler. 2000. An ultrasensitive bacterial motor revealed by monitoring signaling proteins in single cells. *Science.* 287:1652–1655.
37. Vladimirov, N., L. Løvdok, …, V. Sourjik. 2008. Dependence of bacterial chemotaxis on gradient shape and adaptation rate. *PLOS Comput. Biol.* 4:e1000242.
38. Veening, J. W., W. K. Smits, and O. P. Kuipers. 2008. Bistability, epigenetics, and bet-hedging in bacteria. *Annu. Rev. Microbiol.* 62:193–210.